ANALYSIS OF COUPLED BUNCH INSTABILITIES IN THE NSLS-II STORAGE RING WITH A 7-CELL PETRA-III RF STRUCTURE*

G. Bassi†, A. Blednykh, S. Krinsky, J. Rose, BNL, Upton, NY 11973-5000, USA

Abstract

During the commissioning phase 1 of the NSLS-II storage ring an option under consideration is to install a normal conducting 7-cell PETRA-III cavity structure with a stored average current of 25mA. The aim of this paper is to investigate the effect of coupled-bunch instabilities that may be driven by the Higher Order Modes (HOMs) of the 7-cell PETRA-III cavity.

INTRODUCTION

For instability threshold calculations we used the parameters of the bare lattice without damping wigglers and Landau cavities, as given in Table 1. The numerical results discussed in this paper have been obtained with the OASIS (Optimal Algorithm for Self-consistent Instability Simulations) code [1], a recently developed parallel algorithm for self-consistent simulations of single and multi-bunch effects. For single-bunch effects, the code uses the same physical model of the TRANFT code developed by M. Blaskiewicz [2], [6], while in the case of multi-bunch effects the code implements a new self-consistent algorithm to take into account long-range effects [7]. Throughout the paper we restrict our analysis to the case of uniform fillings. First we discuss the longitudinal case for which the analytical theory gives a good estimate of the instability thresholds. The parameters of the longitudinal HOMs are listed in Table 2. Second, we discuss the transverse case and give the parameters of the transverse HOMs, and broadband impedance model as well. We show that the beam is potentially unstable at zero chromaticity. We discuss the beneficial effect of the slow head-tail damping at positive chromaticity on the coupled-bunch instability thresholds, and investigate the HOMs frequencies detuning based upon temperature change as a cure of the coupled-bunch instability. We show that the slow head-tail effect with $N = 3.1 \times 10^8$ particles per bunch ($M = 1320$ bunches, all RF buckets filled), does not provide enough damping to suppress the coupled-bunch instability for values of the chromaticity in the range [0,2]. Since the slow head-tail effect is proportional to the number of particles per bunch, while the coupled-bunch interaction is proportional to the average current $I_0 \propto NM$, to make the slow head-tail effect more effective we discuss fillings with a larger number of particles per bunch, yet below single bunch instability thresholds. Specifically, we consider the case $M = 132$, $N = 3.1 \times 10^9$ and $M = 66$, $N = 6.2 \times 10^9$. A higher number of particles per bunch is limited by the TMCI threshold ($N = 7 \times 10^9$ for the broadband resonator parameters listed in Table 4).

Table 1: Parameters for Threshold Calculations

Parameter	Symbol	Value	Unit
Energy	E	3	GeV
Revolution period	T_0	2.64	μs
Harmonic number	h	1320	
Average current	I_0	25	mA
Momentum compaction	α	3.7×10^{-4}	
Synchrotron tune	ν_s	0.0078	
Average beta function	β_x	8	m
Transverse damping time	τ_x	54	ms
Longitudinal damping time	τ_s	27	ms
Energy spread	$\sigma_{\epsilon 0}$	0.05	
Bunch duration	σ_τ	10	ps

LONGITUDINAL COUPLED-BUNCH ANALYSIS

The longitudinal instability threshold for the NSLS-II storage ring has been analyzed based on numerical data for a 7-cell PETRA-III cavity structure computed by R. Wanzenberg [3]. The longitudinal HOMs parameters are shown in Table 2. The analytical coherent synchrotron frequency Ω_μ of the μth multi-bunch mode is given in [4], [5]. For the dipole mode $a = 1$ and for Gaussian bunches (with uniform filling) the complex coherent frequency shift is given by the Sacherer-Zotter formula

$$\Omega_\mu - \omega_s = i\frac{I_b\alpha}{8\sqrt{\pi}(E_0/e)\sigma_\tau^3\omega_s}\frac{\sum_p \omega' Z_{||}(\omega')e^{-\omega'^2\sigma_\tau^2}}{\sum_p \omega'^2 e^{-\omega'^2\sigma_\tau^2}}$$

where $\omega' = pM\omega_0 + \mu\omega_0 + \omega_s$ and $Z_{||}$ is the total longitudinal impedance of the ring. For $M\omega_0\sigma_\tau \ll 1$ we have $\sum_{p=-\infty}^{+\infty}\omega'^2 e^{-\omega'^2\sigma_\tau^2} \approx \int d\omega\omega^2 e^{-\omega^2}/(M\omega_0\sigma_\tau^3) = \sqrt{\pi}/(2M\omega_0\sigma_\tau^3)$. For our parameters $M\omega_0\sigma_\tau = 0.003$, thus to good approximation we have

$$\Omega_\mu - \omega_s = i\frac{I_b M\alpha}{4\pi(E_0/e)\nu_s}\sum_{p=-\infty}^{+\infty}\omega' e^{-\omega'^2\sigma_\tau^2}Z_{||}(\omega'),$$

and for point bunches

$$\Omega_\mu - \omega_s = i\frac{I_b M\alpha}{4\pi(E_0/e)\nu_s}\sum_{p=-\infty}^{+\infty}(pM\omega_0 + \mu\omega_0 + \omega_s) \times Z_{||}(pM\omega_0 + \mu\omega_0 + \omega_s).$$

In the case of $M = 132$ equally spaced bunches the growth rate $\tau^{-1} = \mathrm{Im}(\Omega - \omega_s)$ of the fastest growing mode

* Work supported by DOE contract DE-AC02-98CH10886
† gbassi@bnl.gov

Table 2: Longitudinal HOMs Parameters of the 7-cell PETRA-III Cavity Structure

f_r, MHz	ω_r, MHz	$R_{sh,\|\|}$,MΩ	$Q_{\|\|}$
500		31.6	36900
501	3147.48	0.0053	37500
502	3154.07	0.0575	38100
503	3160.35	0.0006	38800
505	3172.92	0.0017	39800
507	3185.48	0.0001	40800
508	3191.76	0.0001	41400
712	4473.50	0.0091	30300
716	4498.63	0.0124	31100
722	4536.33	1.13	32300
728	4574.02	3	33600
733	4605.44	0.7245	35000
738	4636.85	0.479	35500
739	4643.14	0.457	36000
1130	7099.79	0.0002	34300
1140	7162.62	0.0008	35500
1150	7225.45	0.0006	37100
1170	7351.11	0.025	38900
1250	7853.75	0.067	55100
1260	7916.58	0.155	55200
1270	7979.41	0.01	49500

Table 3: Transverse HOMs Parameters of the 7-cell PETRA-III Cavity Structure

f_r, MHz	ω_r, MHz	$R_{sh,\perp}$,MΩ/m	$Q_\perp$
860	5403	14.7	55700
867	5447	17.5	56800
869	5460	56.1	58200
871	5473	19.7	59400
1043	6553	83.6	40400
1046	6572	26.2	40900
1089	6842	17.0	49400
1465	9205	15.5	54600
1545	9707	26.8	44300

($\mu = 75$) has been calculated for the sum of longitudinal HOMs from Table 2. The dominant longitudinal HOM has the frequency $\omega_r = 4574.02$MHz and the estimated growth time is 100ms, which is longer than the longitudinal damping time $\tau_s = 27$ms, therefore the beam is stable longitudinally. It should be noted that the numerical simulations of the HOM parameters are done for 7-cell PETRA-III cavity structure with a 40mm beam pipe radius. The regular aperture of the NSLS-II vacuum chamber has an octagonal profile with a 12.5mm vertical half-aperture and with a 38mm horizontal half-aperture. The longitudinal cutoff frequency for the NSLS-II profile ($f_c = 6.8$GHz) is much higher than the cutoff frequency for the beam pipe of the calculated PETRA-III cavity structure ($f_c = 2.9$GHz). This will affect the HOM parameters, such as increasing of shunt impedances and quality factors.

TRANSVERSE COUPLED-BUNCH ANALYSIS

The HOMs parameters for the transverse instability threshold calculations are given in Table 3. In Table 4

Table 4: Impedance Model

PETRA-III cavity HOMs (see Table 2 and 3), $\beta_x = 20$m
Transverse broadband impedance with $f_r = 30$GHz, $R_{sh,\perp} = 1M\Omega/m$, $Q_\perp$=1 and $\bar{\beta}_x = 8$m
792m of aluminum with half-gap of 12.5mm and $\bar{\beta}_x$ = 8m

we list the parameters of the impedance model used. We model the short-range wakefields with a broadband resonator model. Even though we use storage ring parameters without in-vacuum undulators, we include their contribution in the broadband resonator model for an upper estimate. The long-range wakefields are modeled with the HOMS of the PETRA-III cavity and the resistive wall impedance of the alluminum vacuum chamber. An analytical estimate for the coherent frequency shift for Gaussian bunches (with uniform filling) is given by the Sacherer-Zotter formula (for the dipole mode $a = 0$)

$$\Omega_\mu - \omega_\beta = -i\frac{I_b c}{4\sqrt{\pi}\omega_\beta(E_0/e)\sigma_\tau}\frac{\sum_p Z_\perp(\omega')e^{-(\omega'-\omega_\xi)^2\sigma_\tau^2}}{\sum_p \omega'^2 e^{-(\omega'-\omega_\xi)^2\sigma_\tau^2}},$$

where $\omega' = pM\omega_0 + \mu\omega_0 + \omega_\beta$ and $\omega_\xi = \omega_0\xi/\alpha$, and $Z_\perp$ is the total transverse impedance of the ring. Note that the chromaticity is defined as $\xi \equiv \Delta\omega_\beta/(\Delta E/E)$. For $M\omega_0\sigma_\tau \ll 1$ we have that $\sum_{p=-\infty}^{+\infty} e^{-\omega'^2\sigma_\tau^2} \approx \int d\omega e^{-\omega^2}/M\omega_0\sigma_\tau = \sqrt{\pi}/M\omega_0\sigma_\tau$, thus to good approximation we have ($M\omega_0\sigma_\tau = 0.003$)

$$\Omega_\mu - \omega_\beta = -i\frac{I_b M c}{4\pi(E_0/e)\nu_x}\sum_{p=-\infty}^{+\infty} Z_\perp(\omega')e^{-(\omega'-\frac{\xi}{\alpha}\omega_0)^2\sigma_\tau^2},$$

where we used $\nu_x = \omega_\beta/\omega_0$. Clearly for point bunches at zero chromaticity we have the formula

$$\Omega_\mu - \omega_\beta = -i\frac{I_b M c}{4\pi(E_0/e)\nu_x}\sum_{p=-\infty}^{+\infty} Z_\perp(pM\omega_0 + \mu\omega_0 + \omega_\beta).$$

In Fig.1 (top left) we plot the growth rate as a function of mode number μ at chromaticity ξ=0 according to the point bunch formula. The fastest growing mode $\mu = 74$ has a growth time $\tau = 0.74$ms, much smaller than the transverse radiation damping time $\tau_x = 54$ms. Therefore the beam would be unstable at zero chromaticity. In Fig. 1 (top center and top right) we plot the real part of the total impedance $Z_\perp$ evaluated at $\omega(p) = pM\omega_0 + \mu\omega_0 + \omega_\beta$ as a function of p for the fastest growing mode $\mu = 74$. We notice that the dominant contribution to the growth rate comes from the HOM with frequency $\omega_r = 5460$MHz ($f_r = 869$MHz). In our analysis we found that the resistive wall impedance for our chamber with half-gap of 12.5mm has a negligible contribution to the coupled-bunch instability, therefore we drop it from our discussion. At $\xi = 0$ the bunch length σ_τ has a negligible effect on the growth rate and the results are well approximated by the point bunch formula. Since the growth time is $\tau = 0.74$ms at zero chromaticity, we expect the case with $M = 132$ and broadband impedance with parameters as given in Table 4 (we call it Configuration 1) to be unstable at chromaticity 2, in which case the slow head-tail effect provides a damping time of 1.25ms (see Fig. 1, bottom center). To have

ISBN 978-3-95450-115-1

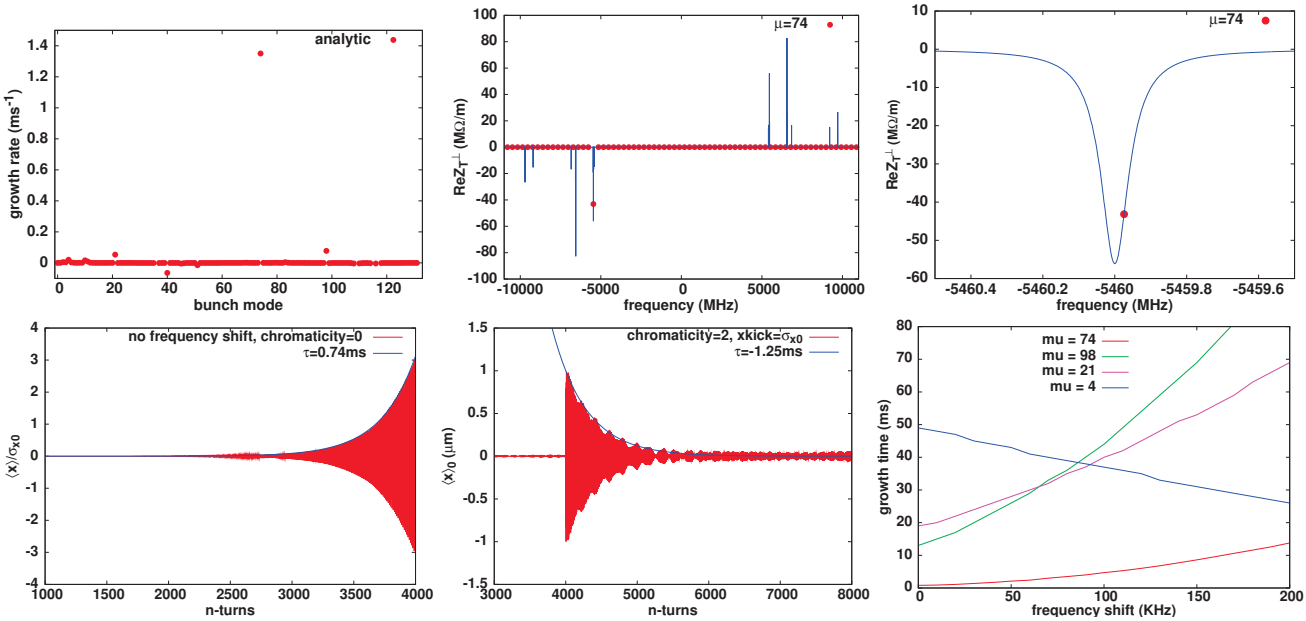

Figure 1: Top left: Growth rates as a function of mode number μ at zero chromaticity. Top center: Real part of $Z_\perp$ evaluated at $pM\omega_0 + \mu\omega_0 + \omega_\beta$ as a function of p for the fastest growing mode $\mu = 74$. Top right: Enlargement of top center figure around the HOM frequency $\omega_r = 5460$MHz. Bottom left: Exponential fit (blue line), using the analytical growth time $\tau = 0.74$ms, of $\langle x\rangle/\sigma_{x0}$ of a single bunch (red line) calculated numerically. Bottom center: Damping time of $\tau = -1.25$ms at $\xi = 2$ provided by the head-tail effect driven by the broadband impedance with parameters as in Table 4. Bottom right: Effect of the frequency shift $\Delta\Omega$ on the growth time of the four fastest growing modes at $\xi = 0$.

Configuration 1 stable at $\xi = 2$, one possibility consists of shifting the frequency of the HOM that is driving the fastest growing mode, without increasing the growth rates of other modes. This can be accomplished by detuning the frequencies of HOMs with a change in the temperature of the cavity. In our simulations we assume that all HOMs are shifted by the same amount $\Delta\Omega > 0$. Our simulations show that Configuration 1 is stable at $\xi = 1$ and $\xi = 2$ for a frequency shift $\Delta\Omega = 60$kHz and $\Delta\Omega = 40$kHz respectively. In Fig.1 (bottom right) we analyze the effect of $\Delta\Omega$ on the growth time of the four fastest growing modes at zero chromaticity. Only the growth time of mode number 4 decreases as $\Delta\Omega$ increases, reaching the value 26ms for $\Delta\Omega = 200$kHz, still above the value 13ms of the mode $\mu = 74$. Since we have chosen the value of $R_{sh,\perp}$=1MΩ/m as an upper estimate for the broadband shunt impedance, we study the case $R_{sh,\perp} = 0.5$MΩ/m as well. We call the case with $M = 132$ and $R_{sh,\perp} = 0.5$MΩ/m Configuration 2. At $\xi = 1$ and $\xi = 2$ we have a stable configuration for $\Delta\Omega = 110$kHz and $\Delta\Omega = 70$ kHz respectively. As expected, since the damping time provided by the slow head-tail instability scales linearly with the shunt impedance, the frequency shift is approximately twice. In a third configuration (Configuration 3), we use the value $R_{sh,\perp} = 0.5$MΩ/m, increasing the number of particles per bunch to $N = 6.2 \times 10^9$, thus decreasing the number of bunches to $M = 66$. Due to the linear dependence of the head-tail damping time on N, at $\xi = 1$ and $\xi = 2$ we have a stable configuration for $\Delta\Omega = 60$kHz and $\Delta\Omega = 40$kHz respectively, as in Configuration 1. To summarize, we have the following working points: Configuration 1 ($M = 132, N = 3.1 \times 10^9$, $R_{sh,\perp} = 1$MΩ/m) is stable at $\xi = 1$ and $\xi = 2$ with a frequency shift of 60kHz and 40kHz respectively, Configuration 2 ($M = 132, N = 3.1 \times 10^9$, $R_{sh,\perp} = 0.5$MΩ/m) is stable at $\xi = 1$ and $\xi = 2$ with a frequency shift of 110kHz and 70 kHz respectively, and Configuration 3 ($M = 66, N = 6.2 \times 10^9$, $R_{sh,\perp} = 0.5$MΩ/m) has the same stability conditions of Configuration 1. Preliminary results from measurements of the HOMs as a function of temperature show that the relation between temperature change and frequency shift for the HOM with frequency $\omega_r = 5460$MHz ($f_r = 869$MHz) is $\Delta f_r = -\alpha\Delta T$, with $\alpha = 10$kHz/°C [8]. Thus a change in the cavity temperature of $\Delta T = -1$°C would induce a frequency shift of Δf_r=10kHz ($\Delta_r\Omega$=62.8kHz), sufficient to stabilize Configuration 1 at chromaticity 2.

REFERENCES

[1] G. Bassi, in preparation.

[2] M. Blaskiewicz, BNL-77074-2006-IR, 2006.

[3] R. Wanzenberg, private communication.

[4] M. Wang, BNL-51302, December 1980.

[5] A. Chao, "Physics of Collective Beam Instabilities in High Energy Accelerators", 1993.

[6] G. Bassi et al., paper THP193, Proceedings of PAC11, New York.

[7] G. Bassi et al., paper TUPPP042, these Proceedings.

[8] Y. Kawashima, unpublished.